Appl Biochem Biotechnol (2012) 166:1533–1551
DOI 10.1007/s12010-012-9548-4

Gold Nanomaterials: Preparation, Chemical Modification, Biomedical Applications and Potential Risk Assessment

Xiu-Mei Jiang · Li-Ming Wang · Jing Wang · Chun-Ying Chen

Received: 23 September 2011 / Accepted: 4 January 2012 /
Published online: 26 January 2012

Abstract Gold nanomaterials (Au NMs) have attracted increasing attention in biomedicine due to their facile preparation, multifunctional modifications, unique optical and electrical properties, and good biocompatibility. The physicochemical properties of Au NMs at nanoscale, like size, shape, surface chemistry, and near field effects, are rendering Au NMs potent candidates in biomedicine. Thus, risk assessment of negative effects of Au NMs on biological systems is becoming urgent and necessary for future applications. In this review, we summarize up-to-date progresses on the preparation and modification of Au NMs and their biomedical applications, including biosensor, bioimaging and phototherapy, gene/drug delivery. Finally, we discuss the potential risk of Au NMs to biological systems, which is instructive for rationally designing and preparing nanomaterials for safe applications in nanomedicine.

Keywords Preparation · Chemical modification · Biosensor · Imaging · Phototherapy · Gene/drug delivery · Risk assessment

Introduction

Materials at nanoscale with special properties like small size effect, quantum effect, and large ratio surface, are quite different from their corresponding bulk materials [1, 2]. With the development of nanoscience and technology, various inorganic nanomaterials including carbon, semiconductor, and metal or metal oxide nanomaterials have been synthesized. Due to unique surface chemical, optical, and electrical properties, Au NMs have attracted great

Authors Xiu-Mei Jiang and Li-Ming Wang contributed equally to this work.

X.-M. Jiang · L.-M. Wang · J. Wang · C.-Y. Chen (✉)
CAS Key Laboratory for Biomedical Effects of Nanomaterials and Nanosafety,
National Center for Nanoscience and Technology, Beijing 100190, China
e-mail: chenchy@nanoctr.cn

L.-M. Wang
Institute of High Energy Physics, Chinese Academy of Sciences, Beijing 100049, China

interest in biomedical applications including biosensor [3], bioimaging and phototherapy [4, 5], gene/drug delivery [6, 7]. Due to localized surface plasmon resonance (LSPR) [8], Au NMs can absorb near infrared (NIR) light efficiently and transfer light to heat, which can be used as bioimaging or photothermal agent for cancer diagnosis and therapy. Au NMs can be used as sensing probes to detect biomolecules via surface enhanced Raman scattering (SERS). Due to their small size, Au NMs can penetrate into cells easily by endocytosis or diffusion, which provides a good chance for gene/drug delivery.

For safe applications in biomedicine, it is critical to clearly understand interactions between Au NMs and biological systems. Their interactions, including cellular uptake, intracellular trafficking and location, cytotoxicity, organ distribution and metabolism, etc. have effects on both biological functions and final fate of Au NMs [9, 10]. As cellular responses to Au NMs can be regulated by controlling their physicochemical properties, synthetic methods have been optimized to control their size, shape, monodispersity, surface charge, and modifications [11–14]. In addition, the acute and chronic toxicity of Au NMs to biological systems and the environment should be evaluated carefully. As was reported, nanomaterials such as carbon nanotubes [15], titanium dioxide nanoparticles [16], copper nanoparticles [17], quantum dots (QDs) [18], and polystyrene (PS) nanoparticles [19] are more or less toxic to biological systems. Although some studies show that Au NMs are biologically safe [20–22], Au NMs can be translocated into the mitochondria and nuclei of cells, causing oxidative stress and genotoxicity [23].

In this review, we summarize the preparation, chemical modification, biomedical applications of Au NMs, and their potential risk to biological systems. We provide an up-to-date review of Au NMs, focusing on the recent development of spherical gold nanoparticles (Au NPs), gold nanorods (Au NRs) and core shell gold nanostructures.

Preparation

Synthetic methods for gold nanostructures are established and optimized. As is shown in Fig. 1, Au NMs in various shapes were synthesized, such as spherical nanoparticles, nanorods, nanoshells, nanocages, and so on [24]. Among these nanostructures, spherical gold nanoparticles and gold nanorods attract the most interest.

There are three main routes to synthesize Au NMs including electrochemical method [25], template method [26–28], and seed-mediated growth method [29] Electrochemical method extended previous studies on the electrochemical synthesis of transition metal clusters within reverse micelles in organic solvent systems [25]. In this synthetic process, the bulk gold metal anode is consumed to form $AuBr_4^-$. These anions complexed with the cationic surfactants migrate to the cathode where reduction occurs. This method provides an available route to prepare high yields of Au NRs [30]. Template method is based on the electrochemical deposition of gold within the pores of nanoporous alumina [31, 32] or polycarbonate template membranes [33]. Kim et al. successfully synthesized highly monodispersed Au NPs with narrow size distribution using surface-functionalized poly (amidoamine) dendrimers as template [34]. This method is controllable and reproducible because the whole process acts in a single aqueous phase. Seed-mediated growth method has the longest history among these three ones. This method is simple and controllable to prepare highly monodispersed Au NMs of various sizes and shapes. There are two basal steps including nucleation and growth. Firstly, gold nanoseeds are prepared by reducing metal salts with a strong reducing agent, and then the growth steps are followed by adding metal salts with a weak reducing agent in the presence of a surfactant [29]. This method was used

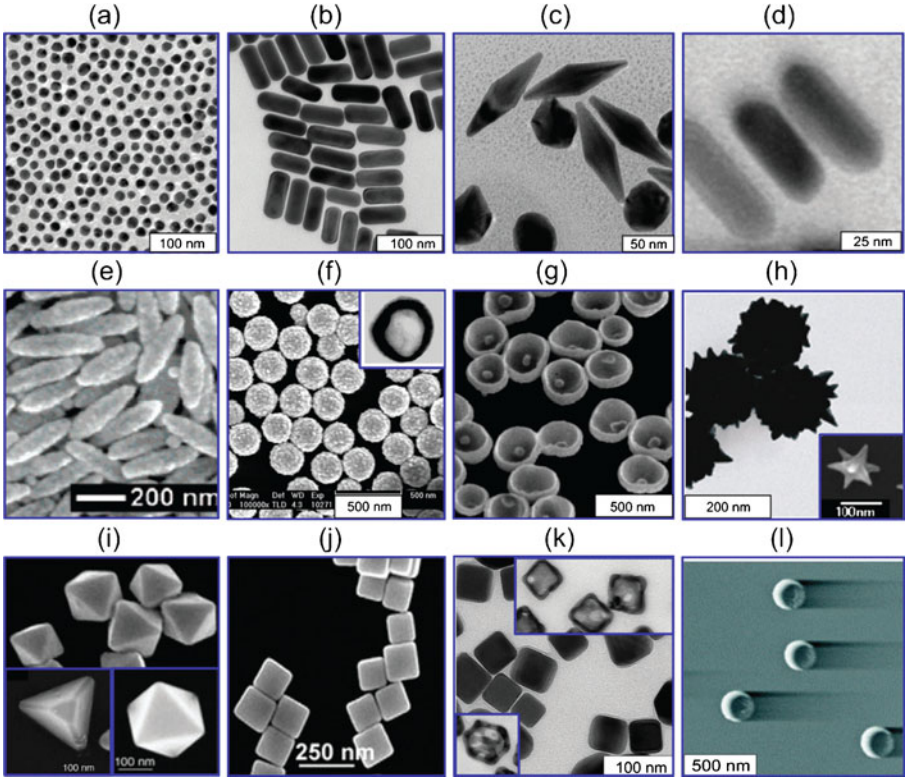

Fig. 1 Various types of plasmon-resonant nanoparticles: 16 nm nanospheres **(a)**; gold nanorods **(b)**; gold bipyramids **(c)**; gold nanorods surrounded by silver nanoshells **(d)**; "nanorice" (gold-coated Fe_2O_3 nanorods) **(e)**; SiO_2/Au nanoshells **(f)** (the *inset* shows a hollow nanoshell); nanobowls with bottom cores **(g)**; spiky SiO_2/Au nanoshells **(h)** (the *inset* shows a gold nanostar); gold tetrahedra, octahedra, and cubooctahedra **(i)**; gold nanocubes **(j)**; silver nanocubes and gold–silver nanocages obtained from them (in the *insets*) **(k)**; and gold nanocrescents **(l)**. Reprinted with permission from reference [24]

to synthesize spherical and non-spherical Au NMs. For example, spherical Au NPs with size ranging from ~10 to 150 nm were obtained by seed-mediated growth method with citrate as a reducing agent [35]. Anisotropic Au NMs are mainly facilitated by adding surfactants such as cetyltrimethylammonium bromide (CTAB), sodium dodecylsulfonate and poly(vinyl-pyrrolidone) to the growth of nuclei or seed particles [36–38].

With respect to Au NMs synthesis, the key point is to control their physicochemical properties. An efficient method to control their size and shape is carried out by controlling the conditions like concentration, surfactant, pH, and temperature in the growth of nanoseeds process [39]. Au NRs with desired quality can be prepared using a hexadecyltrimethylammonium bromide (CTAB)-capped seed instead of citrate-capped one, which decreases the formation of ø-shaped particles and spherical particles [40]. In Fig. 2, Au NRs with different aspect ratios (i.e., the ratio of the length along the long axis to the short axis) were prepared using CTAB as the capping agent [13]. In addition, silver ions can be added in the growth solution to control the length of the Au NRs with aspect ratios ranging from 1.5 to 4.5 [40]. Au NMs fabricated with controlled physicochemical properties will improve their biological applications.

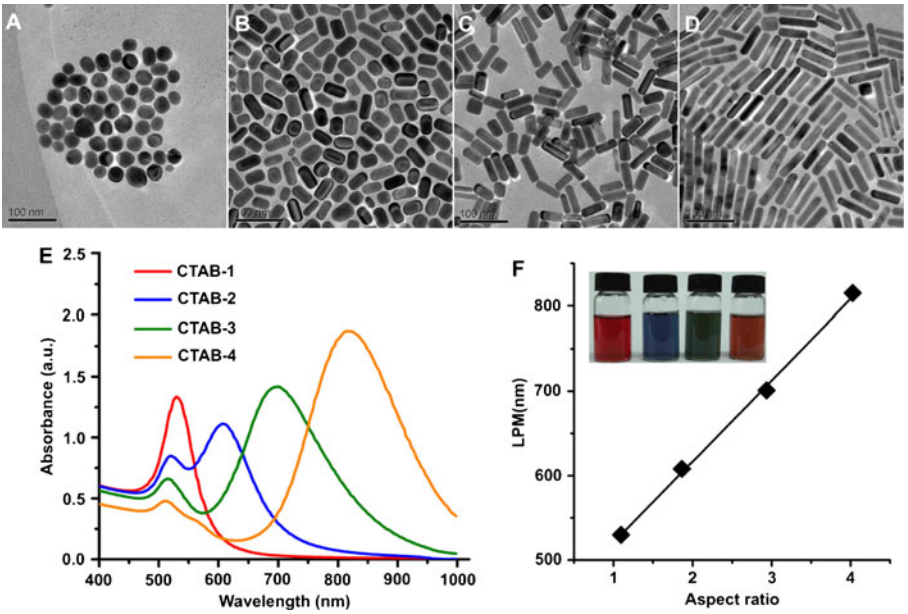

Fig. 2 Characterization of Au NRs. TEM images of CTAB-coated Au NRs with different aspect ratios. **a** CTAB-1, **b** CTAB-2, **c** CTAB-3, and **d** CTAB-4. **e** UV–Vis–NIR absorption spectra of Au NRs. **f** The relationship between longitudinal plasmonic maximum (*LPM*) and calculated aspect ratios (based on TEM images). The *straight line* is a linear regression of data points. The *inset* is the photograph of the Au NRs suspensions with the order of CTAB-1, CTAB-2, CTAB-3, and CTAB-4. The *scale bar*=100 nm. Reproduced with permission from reference [13]

Chemical Modification

Synthesized Au NMs are often coated by citrate or CTAB bilayers, making them well dispersive in aqueous solutions. But they may aggregate when transferred into a cell culture medium since the medium composition is complicated, such as containing salts at high concentration. In addition, CTAB and many other surfactants are found toxic to cells [41]. Surface modifications of Au NMs are necessary for their stability, biocompatibility, functionalization, and targeting. Although Au NMs are inert, they can easily form strong and stable gold–thiolate bonds (Au–S, ~50 kcal/mol). The cross-linking agents contain thiol on one side and carboxyl or amine on the other side. The thiol group binds to the gold surface, and the terminal carboxyl or amine group serves as a binding site to conjugate functional biomolecules such as proteins, peptides, antibodies, DNA or RNA, which enhance dispersibility and render their specific functions of Au NMs [42, 43]. For example, it is an alternative strategy to stabilize citrate or CTAB-capped Au NMs by functionalizing with thiol–PEG [44]. PEG-coated Au NMs showed a nearly neutral surface and had little cytotoxicity in vitro. PEG extends the cycle life of Au NMs in blood, which is helpful for Au NMs accumulating to target tissues for in vivo applications.

Surface modification is also essential for safe and rational applications of Au NMs. Qiu et al. found that Au NRs coated by CTAB could induce serious toxicity to human breast cancer cell line MCF-7, while if further coated by polystyrene sulfonate (PSS) or poly(diallyldimethylammonium chloride) (PDDAC), the cytotoxicity effect decreased greatly [13]. These results suggest that it is very important to utilize surface modifications controlling the

biological effects of Au NMs to satisfy safe applications in nanomedicine. In addition, Partha et al. found that amino acid-functionalized Au NPs provide a scaffold for effective DNA binding with subsequent condensation [45]. Au NPs with lysine and lysine dendron functionality provide highly efficient gene delivery without any observed cytotoxicity. These amino acid-based nanoparticles were sensitive to intracellular glutathione levels, providing a good chance for controlled DNA release and expression. In conclusion, conjugated with proper chemical or biological molecules, Au NMs can perform various functions and their potential effects on biological systems can be also controlled. More detailed information is summarized in Table 1.

Biomedical Applications

The biomedical applications of Au NMs have been developed by improving synthesis and modification methods with desired physicochemical properties and good biocompatibility. Due to small size, large surface ratio and the LSPR of Au NMs provide them unique optical and electrical properties, which can be used for biosensing, bioimaging, gene/drug delivery for cancer diagnosis and therapy. With the aspect ratio of Au NMs increasing, the absorption spectrum maximums shift towards the infrared region, which can be used for phototherapy of cancers because organs and tissues have little absorption within near infrared region.

In the following sections, we will describe the biological applications of Au NMs in different fields separately, including biosensor, bioimaging and phototherapy, and gene/drug delivery.

Biosensor

In order to detect tumor cells in vivo, it is necessary to choose highly sensitive methods to detect and analyze biomarker molecules in human fluid samples and tissue samples. Au NMs provide a good opportunity to detect biomolecules. According to Mie's theory [8], an electromagnetic frequency induces a resonant coherent oscillation of the free electrons called the LSPR. Au NMs exhibit enhanced optical properties due to the LSPR effect. The LSPR depends on the dielectric constant or what is called the refractive index (RI) of the medium surrounding the Au NMs and redshift followed the increase of the medium RI [61–63]. This can be detected by the absorption or scattering microscopy.

The sensitivity of detections is influenced by geometries of nanostructures like the volume, shape, and thickness of shells [64, 65]. For example, Au NRs with an aspect ratio of 3 show six times higher sensitivity than Au NPs [64]. This provides an advantage in applications for multiplexed sensing of different molecules in one solution by using a mixture of nanoparticles with different aspect ratios [66]. Owing to the strong light scattering of Au NMs, dynamic light scattering (DLS) can be a sensitive technique for quantitative detection and analysis of nanoparticle probes at low concentration [3]. For example, one-step homogeneous immunoassay was achieved by using DLS in conjunction with Au NMs as probes. Taking advantage of the large scattering cross section of Au NMs and the high sensitivity of DLS measurement, biomarkers, or other bio-targets can be detected at a very low concentration. In addition, Au NMs can also be a carrier for detectors in the application of biosensing. Specific ligands like chemical or biological molecules could be conjugated with Au NMs for detections. For example, Au NRs conjugated with Pt nanoparticles can be used in ELISA instead of anti-antibody due to the catalase and peroxidase-like activities of

Table 1 Surface functionalities and applications of Au NMs

Au NPs size	Surface functionality	Cell lines/animal studies	Application	Methods	Reference
14, 30, 50, 74, and 100 nm	Citric acid	HeLa cells	Investigate size effect of cellular uptake of Au NMs	ICP-MS	[46]
96.7±2.0 nm	Transferrin	Human nasopharyngeal carcinoma cells (NPC, SUNE1)	Study the cellular uptake process by AFM	AFM	[47]
Length of 55.6±7.8 nm, width of 13.3±1.8 nm	CTAB	Carcinoma cells (A549 cells), normal bronchial epithelial cells (16HBE cells), primary adult stem cells (MSC cells)	Targeting cancer cell damage	TEM, ICP-MS, CLSM	[9]
6 nm, 2 nm	PEI, amino acids	Monkey kidney (COS-7) cells, 293 T cells, monkey kidney cells (Cos-1)	Transfer of plasmid DNA into mammalian cells	TEM, histochemical staining, enzyme activity assay	[45, 48]
2 nm	Mercaptobenzoic acid	Peripheral blood mononuclear			
cells	Effectively inhibits HIV-1 fusion	ELISA	[49]		
2.5±0.4 nm	Tetra(ethylene glycol)	MCF-7 cell	Drug delivery	CLSM, TEM, ICP-MS	[50]
13±1 nm	Oligo nucleotide	RAW 264.7 (macrophage), HeLa (cervical carcinoma), NIH-3 T3 (fibroblast), and MDCK (kidney), lung carcinoma cell line (A549)	Intracellular gene regulation agents for the control of protein expression	Trypan Blue staining, two-photon confocal laser scanning microscopy, CLSM, Western blot	[51, 52]
2–250 nm	Nucleic acid aptamers	HeLa cells	Small-molecule detection	Fluorescence microscopy, flow cytometry,	[53]
13 nm	SiRNA	HeLa cells	RNA interference	CLSM, fluorescence microscopy, flow cytometry	[54]
5, 20, 50, and 100 nm	Oligonucleotide	CCRF-CEM cells (CCL-119 T cell, human acute lymphoblastic leukemia) and Ramos cells (CRL-1596, B cell, human Burkitt's lymphoma)	Cancer cell detection	TEM	[55]
20 nm	Peptide and BSA	HepG2 cells	Nuclear targeting	DLS, gel electrophoresis, fluorescence	[56]

Table 1 (continued)

Au NPs size	Surface functionality	Cell lines/animal studies	Application	Methods	Reference
				spectroscopy, VEC microscopy and DIC microscopy, LDH	
13 nm	Peptide and oligonucleotides	HeLa cells	Antisense gene regulation	Western blots, CLSM	[57]
20 nm	Antibody and oligonucleotides	SiHa and 1483 cell lines	Molecular imaging	MTT assay, DLS, confocal reflectance imaging	[58]
10 nm	Antibody	Breast adenocarcinoma cells (SKBr3)	Cancer cell imaging and therapy	Fluorescence and phase contrast microscopy, SEM, dark field microscopy, NIR laser	[59]
5.6 nm	Lipid	Macrophage cells	Cholesterol binding	CLSM, MRI scanning, gel electrophoresis, TEM, CT	[60]

ICP-MS inductively coupled plasma-mass spectrometry, *AFM* atomic force microscopy, *TEM* transmission electron microscope, *CLSM* confocal laser scanning microscopy, *SEM* scanning electron microscope, *DLS* dynamic light scattering, *VEC* video-enhanced color, *DIC* differential interference contrast, *LDH* lactate dehydrogenase, *MRI* magnetic resonance imaging, *CT* computed tomography, *ELISA* enzyme-linked immunosorbent assay, *MTT* (3-(4,5-dimethylthiazol-2-yl)-2,5-diphenyltetrazolium bromide

Pt nanoparticles (Fig. 3) [67]. In addition, to detect biomolecules, cell-based detection had also been developed. Tan and coworkers used DNA-conjugated Au NPs for cancer cell line (CCRF-CEM) detection through receptor-mediated absorption on the surface of cancer cells [55]. The aptamer-functionalized Au NPs assemble on the surface of cancer cells, causing a redshift in the extinction spectra which can be a direct readout of the target binding by the naked eyes or a spectrometer. These studies point to exciting opportunities in the design of multifunctional Au NMs for early cancer detection and diagnosis.

Imaging and Phototherapy

The plasmon resonance can both radiate light which can be used for optical and imaging and convert light into heat, a process that is useful in phototherapy of cancer. As optical probes, the fluorescence yield efficiency of Au NMs is equivalent to about a million times as that of dye molecules. What is more, Au NMs are photostable and do not undergo photobleaching, showing higher light excitation and energies and longer probing times. In addition, the LSPR absorption spectrum of Au NMs is in the NIR region and can be tuned by changing the size, shape, composition, and environment [68–70], which make them ideal for imaging and thermal therapy of cancer in vivo as tissues are optically transparent in the NIR region.

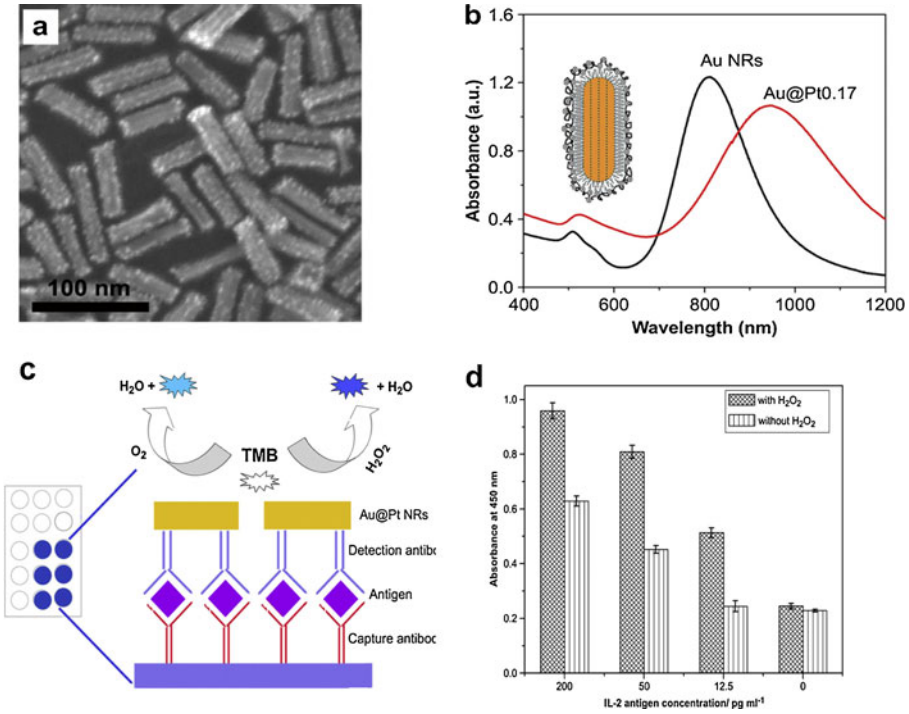

Fig. 3 Au@Pt NRs-based ELISA. SEM image **(a)** and UV–Vis–NIR absorption spectrum **(b)** of Au@Pt nanostructures (*red*) and Au NRs (*blue*) (*inset* is a schematic picture of the nanostructure with *dotted lines* representing Pt nanodots). Antigen is first bounded to capture antibody and then detected by Au@Pt NR-conjugated detection antibody via the oxidation of TMB. Both the oxidase- and peroxidase-like activities of the NRs can be employed **(c)**. Au@Pt 0.17-based ELISA is sensitive to the concentration of mouse IL-2 antigen both in the presence and absence of hydrogen peroxide **(d)**. Reproduced with permission from reference [67]

Conjugated with specific ligands, Au NMs prefer to recognize receptors on the cell membrane and enter cancer cells efficiently through receptor-mediated endocytosis. As is shown in Fig. 4, GNRs was modified with A33scFv through layer by layer method which could be used to selectively kill SW1222 cells by photothermal therapy. In addition, El-Sayed's group used anti-epidermal growth factor receptor (anti-EGFR) antibodies-conjugated Au NRs to detect oral squamous carcinoma cell lines (HSC 313 and HOC 3 Clone 8) and kill them selectively using photothermal effects [71]. They used short NIR laser pulses to irradiate Au NPs; due to strong light scattering from Au NRs in the dark field, the malignant cells are clearly visualized and diagnosed different from the nonmalignant cells by a microscope. It was also found that only half of the power density of the laser is enough to destroy malignant cells than that for nonmalignant cells, which provides a good chance for killing cancer cells efficiently and selectively. In addition, Au NRs have been reported to be able to generate two-photon luminescence at sufficient intensities for single-particle detection and in vivo imaging [5, 72]. The characteristics also provide a chance for real-time imaging of Au NRs accompanying photothermal therapy [73]. Further study revealed that Au NRs can mediate tumor cell death by compromising membrane integrity in thermal therapy. Tong et al. studied the mechanism about the cell damage mediated by phototherapy [74]. Results showed that the most dramatic effect comes from the blebbing of the plasma membrane. It was believed that the membrane blebbing was due to the disruption of actin filaments, resulting in Ca^{2+} influx and the depolymerization of the intracellular actin network.

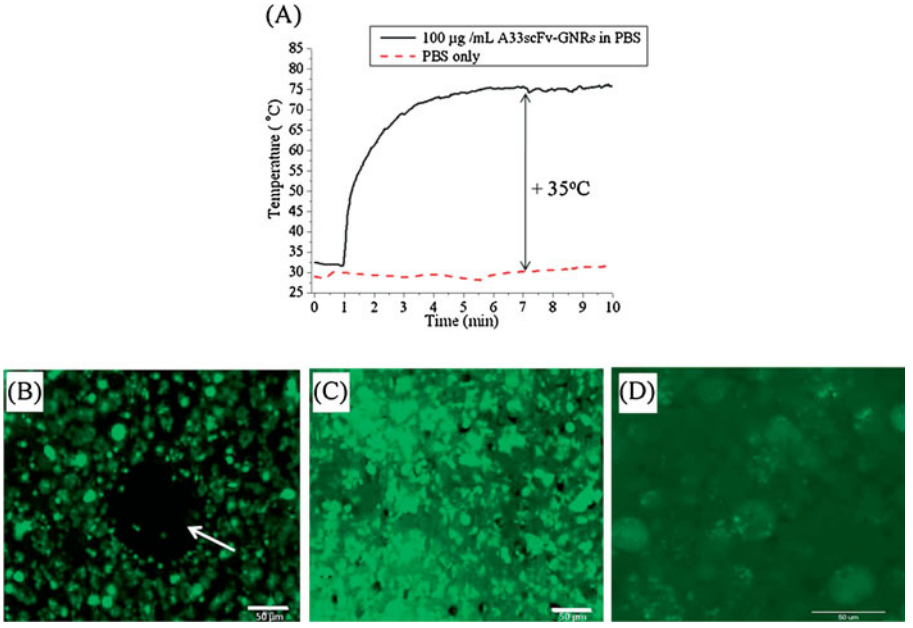

Fig. 4 Au NR-assisted photothermal therapy of colorectal carcinoma cells irradiated by 808 nm NIR laser. **a** Graph shows 35 °C temperature increase in an A33scFv-Au NRs solution (100 mL, 100 mg mL^{-1}) when irradiated by an 808-nm laser. **b** SW 1222 cells incubated with A33scFv-Au NRs. **c** SW1222 cells pretreated with excess A33scFv before addition of A33scFv-Au NRs. **d** HT 29 cells incubated with A33scFv-Au NRs followed by laser irradiation. Nanorods are incubated for 5 h, and laser treatment is performed at 5.1 $W cm^{-2}$ power density. Viable cells appear *green* due to calcein/AM staining while *dark areas* devoid of fluorescence are cells destroyed from photothermal therapy irradiation. *Scale bar* is 50 μm. Reproduced with permission from reference [94]

The many examples discussed above illustrate the exciting potential of using functionalized Au NMs for cancer diagnosis and therapy, by coupling biomedical imaging with photothermal therapy to provide a noninvasive alternative to surgery for cancer treatments.

Gene/Drug Delivery

It is becoming feasible to regulate cellular behavior like enhanced secretion of specific molecules, proliferation, and differentiation by delivering gene/drugs into cells. One of the current challenges is how to deliver specific gene/drugs into cells or organelles efficiently and targetedly. Therefore, building an efficient delivery system is imperative under the situation. An ideal delivery system should allow efficient cell entrance, protection of gene/drugs from degradation by nucleases or proteases, and release of drug/genes in functional form into desired organelles.

Recently, organic and inorganic nanomaterials interacting with biological systems has attracted great interest in the field of biomedicine. Some of these delivery systems like silica nanoparticles, QDs, micelles, dendrimers, liposomes, molecular conjugates, and ultrasound microbubbles have been extensively investigated for drug/gene delivery [75–79]. Due to small size, facile synthesis [2, 11, 35, 80–82], controllable modification, and good biocompatibility, Au NMs have emerged as an attractive candidate for the delivery of various payloads into their targets [83, 84]. For example, Au NMs efficiently condense drug concentration by conjugating many molecules on one gold core. A single Au NP with a 2-nm core diameter could be conjugated with about 100 molecules in principle to available ligands (n = ~108) in the monolayer [85]. The payloads could be large biomolecules like DNA [51, 86], RNA [87] or proteins [88], and also small molecules. Furthermore, the prerequisite of delivery is how to release the carried molecules efficiently. A controlled release which depends on pH [89, 90] and light [91] provide efficient ways to make drugs/genes function. As is shown in Fig. 5, Rotello et al. used cationic Au NPs to deliver DNA into the nucleus of mouse embryonic fibroblast cell lines [92]. They found that cationic Au NPs provide an efficient platform for DNA surface binding. One positively charged Au NP bearing a photoactive o-nitrobenzyl ester linkage, which allows temporal and spatial release of DNA by near-UV irradiation (>350 nm). This reversal in electrostatics leads to the efficient release of DNA from the nanoparticle, resulting in a high level of recovery of DNA transcription in vitro.

Currently, Au NMs have emerged as a promising platform for drug and gene delivery. Their properties including low cytotoxicity, high surface area, and tunable stability are favorable for their applications in delivery. Moreover, the delivery efficiency could be influenced by the size, shape, surface charge, and modifications of Au NMs, which should be considered for the rational design of Au NMs as carriers.

Potential Risk Assessment

Considering biological applications, the interactions of Au NMs with cells have been explored [9, 13, 93, 94]. Results showed that Au NMs absorb proteins from fetal bovine serum quickly after they are incubated with cell culture medium, forming a protein–nanoparticle corona, which can be internalized by cells through receptor or non-receptor mediated endocytosis and then translocated to endosomes or lysosomes in most cases. Very few Au NMs cause cytotoxicity if not entering the cytoplasm or nucleus. Furthermore, metabolic kinetics of Au NMs at animal level has also been studied, as biokinetic study is a fundamental step to evaluate safe and sustainable use of nanoparticles. Wang et al. found that Au NRs have a short half-life in blood

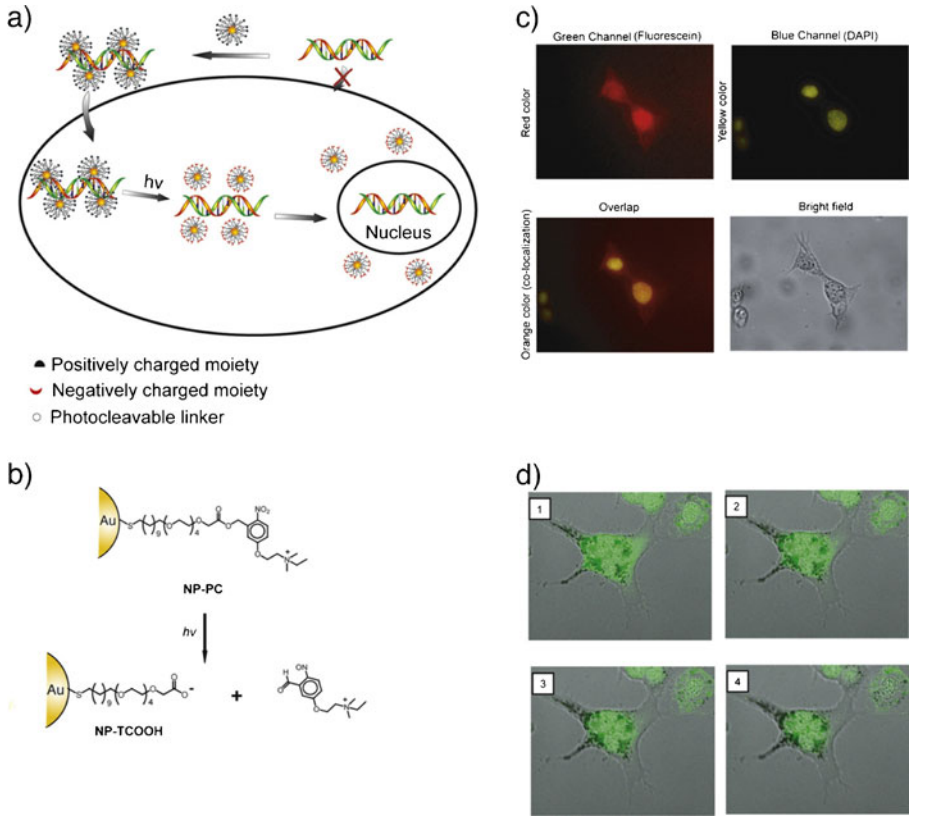

Fig. 5 **a** Schematic illustration for nuclear delivery and light-regulated release of DNA using photolabile nanoparticles. **b** Light-induced surface transformation of GNP-PC. **c** Fluorescence and bright field microscopy images after photo inducing release of DNA from the GNP-PC–DNA complex. *Green channel* (fluorescein) and *blue channel* (DAPI) are depicted with *red* and *yellow*, respectively. **d** Confocal micrographs illustrating the accumulation of photo-released DNA inside the nucleus. *Panels 1*, *2*, *3* and *4* show four images for consecutive slices of z-series (interval=1.0 μm). Reproduced with permission from reference [86]

circulation and mainly accumulated in the liver, spleen, and lung of the mouse [10]. There is a size-dependent effect on the organ distribution of Au NPs. After intravenous injection of Au NPs with different sizes into animals for 24 h, quantification of gold by inductively coupled plasma-mass spectrometry showed that Au NMs with a size of 10 nm exhibiting the most widespread distribution in organs including blood, the liver, spleen, kidney, testis, thymus, heart, lung, and brain than Au NMs with sizes at 50, 100, and 250 nm [95]. As long-term accumulation of Au NMs in the liver and spleen and other organs may cause negative effects on their biological functions, rational design on size and surface modification of Au NMs should be taken into consideration for long life cycle and low toxicity in vivo.

Since Au NMs have promising applications in biomedicine, more attention should be paid to potential risk assessment of nanomaterials to human health and the environment. With a small size, Au NMs can easily enter cells by endocytosis or direct penetration. However, the latter process may cause serious toxicity by compromising the cell membrane. Cytotoxicity was influenced by the physicochemical properties of Au NMs like size [96], surface charges [97], and modifications [9, 13].

Pan et al. studied the size-dependent effect on cytotoxicity. They varied particle sizes from 0.8 to 15 nm and studied their cytotoxicity on four cell lines including cervix carcinoma epithelial cells (HeLa), melanoma cells (SK-Mel-28), mouse fibroblasts (L929), and mouse monocytic/macrophage cells (J774A1). Results showed that cellular response is size dependent. Au NPs with a size of 1–2 nm were highly toxic and the same as gold compounds, while those larger than 15 nm were relatively nontoxic. In addition, they also found that the toxicity of different size shows in different ways, particles of 1.4 nm cause predominantly rapid cell death by necrosis within 12 h, while closely related particles of 1.2 nm induce programmed cell death by apoptosis [96]. They suggest that Au NPs with different sizes have different interaction mechanisms with cell membrane, causing difference in cytotoxicity.

Besides size, surface charge also has influences on their cytotoxicity. As we know, cell membrane is negatively charged, so cationic Au NPs easily absorb onto the cell membrane than the anionic ones [97]. It was reported that the internalization rate of cationic Au NPs is five times higher than that of anionic ones due to different uptake pathways. It is regarded

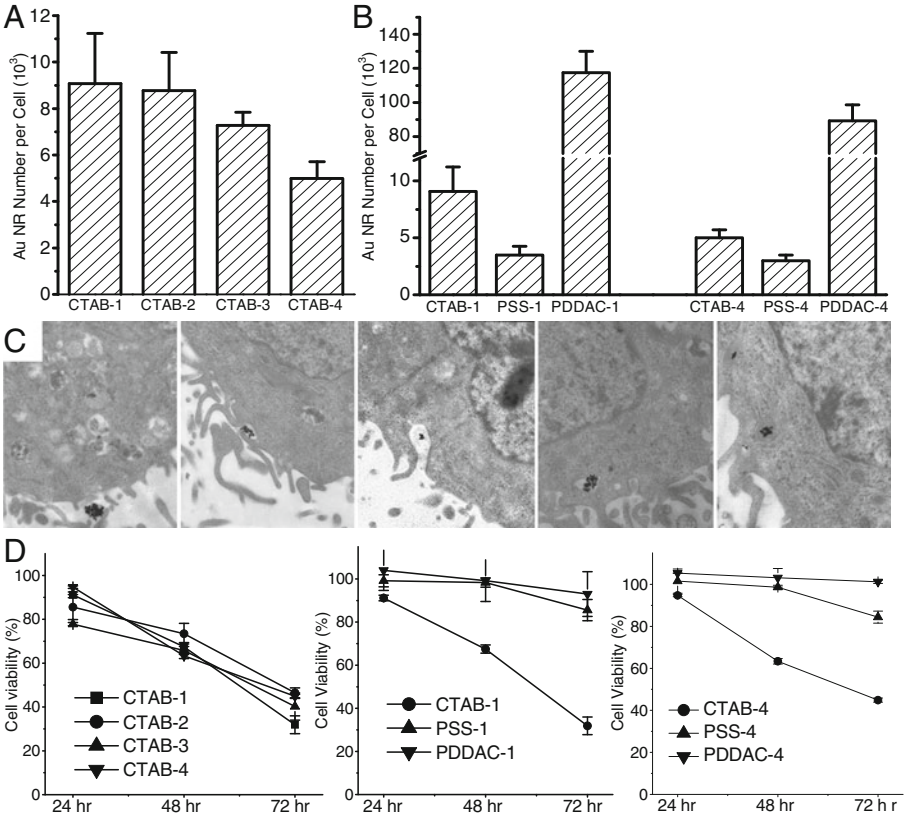

Fig. 6 Surface chemistry and aspect ratio-mediated uptake of Au NRs. **a** Cellular uptake of Au NRs by MCF-7 cells with different aspect ratios from 1 to 4: CTAB-1, CTAB-2, CTAB-3, and CTAB-4. **b** The shape and surface coating influencing cellular uptake of Au NRs. **c** TEM images showing the process of cellular uptake. The Au NRs form aggregates, enter into vesicles and further get into lysosomes. **d** Cytotoxicity of Au NRs after 24, 48, and 72 h treatment using CTAB-capped Au NRs with different aspect ratios (*left inset*) and using Au NRs with different surface coatings (*middle* and *right insets*). Reproduced with permission from reference [13]

that anionic Au NPs are probably internalized by endocytosis, while cationic ones directly penetrate into cells by disrupting the membrane, which causes serious cytotoxicity.

What is more, surface modifications have a vital influence on their cytotoxicity. As is shown in Fig. 6, CTAB-capped Au NRs were found to be toxic to human breast cancer MCF-7 [98]. However, if being further coated with PSS or PDDAC, their cytotoxicity decreases greatly [13]. In addition, cell types also determine cell responses to Au NMs. As is shown in Fig. 7, our recent work has uncovered that CTAB-stabilized Au NRs can selectively target the mitochondria in cancer cells (carcinoma A549) and finally kill them while have negligible effects on

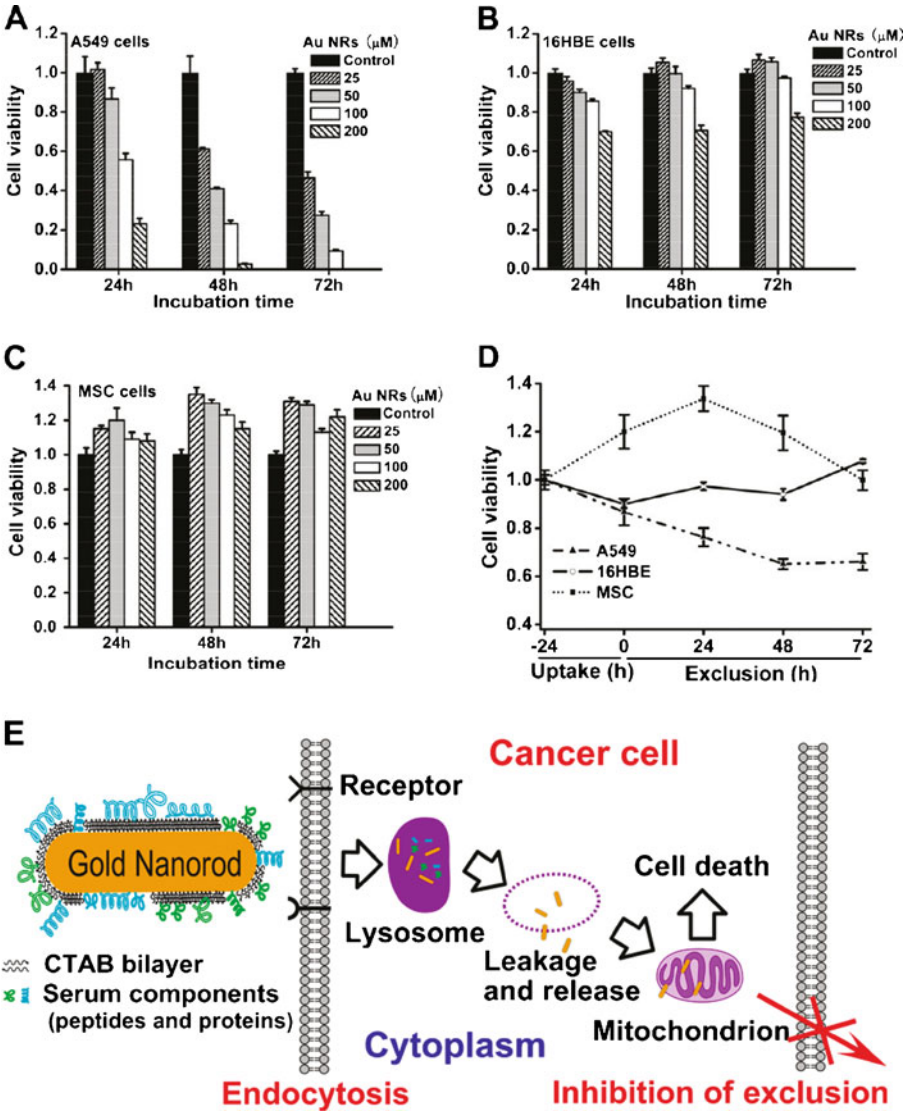

Fig. 7 The changes in cell viability and actin cytoskeletons during uptake and removal of Au NRs. **a–c** Cell viability in A549, 16HBE, and MSC cells determined by the CCK-8 assay after their exposure to Au NRs. **d** Cell viability during cellular uptake and exclusion of Au NRs. **e** The proposed mechanism how Au NRs selectively kill cancer cells. Reproduced with permission from reference [9]

Table 2 Toxic effects of Au NMs with different physiochemical properties to biological systems

Size	Surface properties	Cell type, animals	Exposure	Toxicity	Method	Reference
7 nm	PVP	HEK293, MDA-MB-231	10, 25, 50, 100 μM; 24 h	Non-cytotoxicity.	MTT	[20]
4, 12, 18 nm	Citrate, Biotin, L-cysteine, Glucose, CTAB	K562	0–250 μM (Au atoms); 3 days	Citrate and biotin coatings show negligible toxicity at 250 μM; glucose and cysteine-modified Au NPs are not toxic up to 25 μM; 18-nm CTAB-coated Au NPs display significant toxicity	MTT	[98]
13±1 nm	Citrate	Human dermal fibroblasts	0–0.8 mg/mL; 2–6 days	Cell volume, density, morphology, and actin stress fibers decrease and vacuoles increase with large dose of Au NPs	Confocal microscopy, AFM, TEM	[99]
15 nm	BSA	NIH-3 T3	0.1, 1, 10, 100 μM; 3 h	100% viability	MTT	[21]
N/A	PEI	COS-7	N/A; 6 h	Enhance transfect efficiency but decrease 20–30% viability after transfection	MTT	[48]
15×58 nm	CTAB, PEG-SH	A549, 16HBE, MSC	50–200 μM (gold amount); 24, 48, 72 h	CTAB-coated Au NRs kill A549 while pose negligible impact on 16HBE and MSC cells. PEG-Au NRs have negligible toxicity.	CCK-8, confocal microscopy	[9]
3–8 nm	Lysine, PLL, FITC	RAW264.7	10, 25, 50, and 100 μM; 24, 48, 72 h	Reduce the production of reactive oxygen and nitrite species, and do not elicit secretion of proinflammatory cytokines TNF-α and IL1-β.	MTT	[100]
45×18 nm, 40×12 nm	PSS, PEG-SH	SKBR3, CHO, C2C12, HL60	20–174 pM; 24 h	PSS showed substantial cytotoxicity Only HL60 showed a toxic	MTT	[101]

Table 2 (continued)

Size	Surface properties	Cell type, animals	Exposure	Toxicity	Method	Reference
				response at high concentrations of the PEGylated particles		
3, 5, 8, 12, 17, 37, 50, 100 nm	BSA, lysozyme, peptides	Mice	8 mg/kg/week, 50 days	Au NPs of 3, 5, 50, and 100 nm did not show harmful effects, but 8 to 37 nm induced severe sickness in mice	MTT, histology, CARS microscopy	[102]
13 nm	PEG-SH	Mice	0.17, 0.85, 4.26 mg/kg; 5, 30 min; 4, 24 h; and 7 days	Induce acute inflammation and apoptosis in the liver	ICP-MS, histology, TEM	[103]
4 nm, 100 nm	PEG-SH	Mice	4.26 mg/kg; 30 min	Only 0.38% (170 genes) and 0.50% (224 genes) of the total genes (45,000 genes) were significantly reduced by the treatment of 4 or 100 nm Au NPs	Histology, TEM, TUNEL assay	[104]
20 nm		Rats	0.01–0.015 mg/kg; 1, 7 days; 1 and 2 months	Microarray results of liver and spleen demonstrate significant effects on genes related to detoxification, lipid metabolism, cell cycle, defense response, and circadian rhythm	RNA microarray analyses	[105]
12.5 nm		Mice	40, 200, 400 mg/kg/day; 8 days	No evidence of toxicity	Histology, serum, biochemical analysis, hematological analysis	[22]

PVP poly(vinylpyrrolidone), *ICP-MS* inductively coupled plasma-mass spectrometry, *TNF* tumor necrosis factor, *IL* interleukin, *TUNEL* terminal deoxynucleotidyl transferase dUTP nick end labeling, *AFM* atomic force microscopy, *TEM* transmission electron microscope, *CARS* coherent anti-Stokes Raman scattering, *MTT* (3-(4,5-dimethylthiazol-2-yl)-2,5-diphenyltetrazolium bromide

normal human bronchial epithelial cells (16HBE) and bone marrow mesenchymal stem cells (MSC), which provide an opportunity for selective cancer therapy [9]. The mechanism was supposed that CTAB-coated Au NRs can be released from the lysosomes and translocated into the mitochondria of cancer cells while stay in the lysosomes in normal cells or excluded out of the stem cells, which cause the mitochondrial membrane potential to decrease and the reactive oxygen species to increase, inducing cancer cell death while they have negligible effects on normal and stem cells.

Another important factor for risk assessment is concentration or dose. Almost everything is toxic if the dose ran out. It was found that 50 μM of CTAB-capped Au NRs cause half death of HepG2 cells, and cell viability decreases with increased concentration of Au NRs [9].

In Table 2, we summarize different physicochemical properties of Au NMs and their potential toxicity to biological systems. As size, surface properties, and cell types affect biological responses to Au NMs, it is difficult to make a clear and consensus conclusion on toxicity of Au NMs. But what we can do is synthesizing biocompatible Au NMs and modifying them with biocompatible molecules to make them safe for biological systems. Although Au NMs show cytotoxicity in some cases, the advantage is that we could do something to reduce or shield the toxicity. On the other hand, we can make use of their cytotoxic effects in cancer therapy by selectively targeting cancer cells and inducing cell death.

Conclusion and Perspective

To conclude, Au NMs are becoming promising stars in biomedical applications because of their unique properties and advantages as below. Firstly, most Au NMs can be synthesized easily and conveniently, not relying on complicated equipment and technologies. Secondly, Au NMs are relatively inert and can be functionalized by various chemical or biological molecules, which make them biocompatible and multifunctional. Thirdly and the most important point is that Au NMs have unique optical and electrical properties, like localized surface plasmon resonance, making them ideal materials for biological detection and cancer therapy. With the improvement of methods on fabrication, modification, and functionalization, Au NMs will provide more advantages for biological applications. However, their potential risk to human and the environment should be commented cautiously before applications. So far, we have not made a consistent conclusion on the toxicity of Au NMs. Because materials of different sizes, shapes, surface charges, and surface modifications as well as cell types were used in experiments. What should be done next is to establish standard methods and evaluation systems to predict their cytotoxicity and biological effects. On the other hand, considering for safe biomedical applications, their long-term effects and final fates of Au NMs in an organism should be carefully studied.

Acknowledgments This work was supported by the MOST 973 Program (2011CB933401 and 2012CB934003), the NSFC (31070854), and CAS Knowledge Innovation Projects.

References

1. Nie, S., & Emory, S. R. (1997). *Science, 275*, 1102–1106.
2. Schmid, G. (1992). *Chemical Reviews, 92*, 1709–1727.
3. Liu, X., Dai, Q., Austin, L., Coutts, J., Knowles, G., Zou, J., et al. (2008). *Journal of the American Chemical Society, 130*, 2780–2782.

4. Durr, N. J., Larson, T., Smith, D. K., Korgel, B. A., Sokolov, K., & Ben-Yakar, A. (2007). *Nano letters, 7*, 941–945.
5. Imura, K., Nagahara, T., & Okamoto, H. (2005). *The Journal of Physical Chemistry B, 109*, 13214–13220.
6. Salem, A. K., Searson, P. C., & Leong, K. W. (2003). *Nature Materials, 2*, 668–671.
7. Chen, C.-C., Lin, Y.-P., Wang, C.-W., Tzeng, H.-C., Wu, C.-H., Chen, Y.-C., et al. (2006). *Journal of the American Chemical Society, 128*, 3709–3715.
8. Mie, G. (1908). *Annalen der Physik, 330*, 377–445.
9. Wang, L., Liu, Y., Li, W., Jiang, X., Ji, Y., Wu, X., et al. (2011). *Nano letters, 11*, 772–780.
10. Wang, L., Li, Y. F., Zhou, L., Liu, Y., Meng, L., Zhang, K., et al. (2010). *Analytical and Bioanalytical Chemistry, 396*, 1105–1114.
11. Grabar, K. C., Freeman, R. G., Hommer, M. B., & Natan, M. J. (1995). *Analytical chemistry, 67*, 735–743.
12. Busbee, B. D., Obare, S. O., & Murphy, C. J. (2003). *Advanced Materials, 15*, 414–416.
13. Qiu, Y., Liu, Y., Wang, L., Xu, L., Bai, R., Ji, Y., et al. (2010). *Biomaterials, 31*, 7606–7619.
14. Khlebtsov, N., & Dykman, L. (2011). *Chemical Society Reviews, 40*, 1647–1671.
15. Zhao, Y., Xing, G., & Chai, Z. (2008). *Nature Nanotechnology, 3*, 191–192.
16. Wang, J., Zhou, G., Chen, C., Yu, H., Wang, T., Ma, Y., et al. (2007). *Toxicology letters, 168*, 176–185.
17. Chen, Z., Meng, H., Xing, G., Chen, C., Zhao, Y., Jia, G., et al. (2006). *Toxicology letters, 163*, 109–120.
18. Qu, Y., Li, W., Zhou, Y., Liu, X., Zhang, L., Wang, L., et al. (2011). *Nano letters, 11*, 3174–3183.
19. Liu, Y., Li, W., Lao, F., Liu, Y., Wang, L., Bai, R., et al. (2011). *Biomaterials, 32*, 8291–8303.
20. Zhou, M., Wang, B., Rozynek, Z., Xie, Z., Fossum, J. O., Yu, X., et al. (2009). *Nanotechnology, 20*, 505606–505615.
21. Murawala, P., Phadnis, S., Bhonde, R., & Prasad, B. (2009). *Colloids and Surfaces B: Biointerfaces, 73*, 224–228.
22. Lasagna-Reeves, C., Gonzalez-Romero, D., Barria, M. A., Olmedo, I., Clos, A., & Sadagopa Ramanujam, V. M. (2010). *Biochemical and Biophysical Research Communications, 393*, 649–655.
23. Li, J. J., Zou, L., Hartono, D., Ong, C. N., Bay, B. H., & Lanry Yung, L. Y. (2008). *Advanced Materials, 20*, 138–142.
24. Dykman, L., & Khlebtsov, N. (2011). *Chem Soc Rev.* doi:10.1039/c1cs15166e.
25. El-Sayed, I. H., Huang, X., & El-Sayed, M. A. (2005). *Nano letters, 5*, 829–834.
26. Martin, C. R. (1994). *Science, 266*, 1961–1966.
27. Foss, C. A., Jr., Hornyak, G. L., Stockert, J. A., & Martin, C. R. (1992). *The Journal of Physical Chemistry, 96*, 7497–7499.
28. Martin, C. R. (1996). *Chemistry of Materials, 8*, 1739–1746.
29. Jana, N. R., Gearheart, L., & Murphy, C. J. (2001). *The Journal of Physical Chemistry B, 105*, 4065–4067.
30. Yu, Y. Y., Chang, S. S., Lee, C. L., & Wang, C. R. C. (1997). *The Journal of Physical Chemistry B, 101*, 6661–6664.
31. Martin, B. R., Dermody, D. J., Reiss, B. D., Fang, M., Lyon, L. A., Natan, M. J., et al. (1999). *Advanced Materials, 11*, 1021–1025.
32. van der Zande, B. M. I., Böhmer, M. R., Fokkink, L. G. J., & Schönenberger, C. (2000). *Langmuir, 16*, 451–458.
33. Penner, R. M., & Martin, C. R. (1987). *Analytical Chemistry, 59*, 2625–2630.
34. Kim, Y.-G., Oh, S.-K., & Crooks, R. M. (2003). *Chemistry of Materials, 16*, 167–172.
35. Frens, G. (1973). *Nature, 241*, 20–22.
36. Kuo, C. H., Chiang, T. F., Chen, L. J., & Huang, M. H. (2004). *Langmuir, 20*, 7820–7824.
37. Kwon, K., Lee, K. Y., Lee, Y. W., Kim, M., Heo, J., Ahn, S. J., et al. (2007). *The Journal of Physical Chemistry C, 111*, 1161–1165.
38. Kan, C., Wang, C., Zhu, J., & Li, H. (2010). *Journal of Solid State Chemistry, 183*, 858–865.
39. Nguyen, D. T., Kim, D.-J., & Kim, K.-S. (2011). *Micron, 42*, 207–227.
40. Nikoobakht, B., & El-Sayed, M. A. (2003). *Chemistry of Materials, 15*, 1957–1962.
41. Alkilany, A. M., Nagaria, P. K., Hexel, C. R., Shaw, T. J., Murphy, C. J., & Wyatt, M. D. (2009). *Small, 5*, 701–708.
42. Daniel, M. C., & Astruc, D. (2004). *Chemical Reviews, 104*, 293–346.
43. Rosi, N. L., & Mirkin, C. A. (2005). *Chemical Reviews, 105*, 1547–1562.
44. Niidome, T., Yamagata, M., Okamoto, Y., Akiyama, Y., Takahashi, H., Kawano, T., et al. (2006). *Journal of Controlled Release, 114*, 343–347.
45. Ghosh, P. S., Kim, C.-K., Han, G., Forbes, N. S., & Rotello, V. M. (2008). *ACS Nano, 2*, 2213–2218.
46. Chithrani, B. D., Ghazani, A. A., & Chan, W. C. W. (2006). *Nano letters, 6*, 662–668.
47. Yang, P.-H., Sun, X., Chiu, J.-F., Sun, H., & He, Q.-Y. (2005). *Bioconjugate Chemistry, 16*, 494–496.

48. Thomas, M., & Klibanov, A. M. (2003). *Proceedings of the National Academy of Sciences, 100*, 9138–9143.
49. Bowman, M. C., Ballard, T. E., Ackerson, C. J., Feldheim, D. L., Margolis, D. M., & Melander, C. (2008). *Journal of the American Chemical Society, 130*, 6896–6897.
50. Kim, C. K., Ghosh, P., Pagliuca, C., Zhu, Z. J., Menichetti, S., & Rotello, V. M. (2009). *Journal of the American Chemical Society, 131*, 1360–1361.
51. Rosi, N. L., Giljohann, D. A., Thaxton, C. S., Lytton-Jean, A. K. R., Han, M. S., & Mirkin, C. A. (2006). *Science, 312*, 1027–1030.
52. Seferos, D. S., Giljohann, D. A., Rosi, N. L., & Mirkin, C. A. (2007). *Chem Bio Chem, 8*, 1230–1232.
53. Zheng, D., Seferos, D. S., Giljohann, D. A., Patel, P. C., & Mirkin, C. A. (2009). *Nano letters, 9*, 3258–3261.
54. Giljohann, D. A., Seferos, D. S., Prigodich, A. E., Patel, P. C., & Mirkin, C. A. (2009). *Journal of the American Chemical Society, 131*, 2072–2073.
55. Medley, C. D., Smith, J. E., Tang, Z., Wu, Y., Bamrungsap, S., & Tan, W. (2008). *Analytical chemistry, 80*, 1067–1072.
56. Tkachenko, A. G., Xie, H., Coleman, D., Glomm, W., Ryan, J., Anderson, M. F., et al. (2003). *Journal of the American Chemical Society, 125*, 4700–4701.
57. Patel, P. C., Giljohann, D. A., Seferos, D. S., & Mirkin, C. A. (2008). *Proceedings of the National Academy of Sciences, 105*, 17222–17226.
58. Nitin, N., Javier, D. J., & Richards-Kortum, R. (2007). *Bioconjugate Chemistry, 18*, 2090–2096.
59. Loo, C., Lowery, A., Halas, N., West, J., & Drezek, R. (2005). *Nano letters, 5*, 709–711.
60. Cormode, D. P., Skajaa, T., Van Schooneveld, M. M., Koole, R., Jarzyna, P., Lobatto, M. E., et al. (2008). *Nano letters, 8*, 3715–3723.
61. Haes, A. J., & Van Duyne, R. P. (2002). *Journal of the American Chemical Society, 124*, 10596–10604.
62. Lee, K. S., & El-Sayed, M. A. (2006). *The Journal of Physical Chemistry B, 110*, 19220–19225.
63. Underwood, S., & Mulvaney, P. (1994). *Langmuir, 10*, 3427–3430.
64. Perez-Juste, J., Pastoriza-Santos, I., Liz-Marzan, L. M., & Mulvaney, P. (2005). *Coordination Chemistry Reviews, 249*, 1870–1901.
65. Jain, P. K., & El-Sayed, M. A. (2007). *The Journal of Physical Chemistry C, 111*, 17451–17454.
66. Yu, C., & Irudayaraj, J. (2007). *Analytical chemistry, 79*, 572–579.
67. He, W., Liu, Y., Yuan, J., Yin, J. J., Wu, X., Hu, X., et al. (2010). *Biomaterials, 32*, 1139–1147.
68. Kelly, K. L., Coronado, E., Zhao, L. L., & Schatz, G. C. (2003). *The Journal of Physical Chemistry B, 107*, 668–677.
69. Link, S., & El-Sayed, M. A. (2000). *International Reviews in Physical Chemistry, 19*, 409–454.
70. Oldenburg, S., Averitt, R., Westcott, S., & Halas, N. (1998). *Chemical Physics Letters, 288*, 243–247.
71. El-Sayed, I. H., Huang, X., & El-Sayed, M. A. (2006). *Cancer Letters, 239*, 129–135.
72. Wang, H., Huff, T. B., Zweifel, D. A., He, W., Low, P. S., Wei, A., et al. (2005). *PNAS, 102*, 15752–15756.
73. Huff, T. B., Tong, L., Zhao, Y., Hansen, M. N., Cheng, J. X., & Wei, A. (2007). *Nanomedicine, 2*, 125–132.
74. Tong, L., Zhao, Y., Huff, T. B., Hansen, M. N., Wei, A., & Cheng, J. X. (2007). *Advanced Materials, 19*, 3136–3141.
75. Panyam, J., & Labhasetwar, V. (2003). *Advanced Drug Delivery Reviews, 55*, 329–347.
76. Liu, Y., Chen, X., & Xin, J. (2006). *Journal of materials science, 41*, 5399–5401.
77. Liu, Y., Miyoshi, H., & Nakamura, M. (2006). *Journal of controlled release, 114*, 89–99.
78. Okuda, T., Kawakami, S., Akimoto, N., Niidome, T., Yamashita, F., & Hashida, M. (2006). *Journal of controlled release, 116*, 330–336.
79. Moghimi, S., & Szebeni, J. (2003). *Progress in lipid research, 42*, 463–478.
80. Turkevich, J., Stevenson, P. C., & Hillier, J. (1951). *Discussions of the Faraday Society, 11*, 55–75.
81. Brust, M., Walker, M., Bethell, D., Schiffrin, D., & Whyman, R. (1994). *Journal of the Chemical Society, Chemical Communications, 7*, 801–802.
82. Templeton, A. C., Wuelfing, W. P., & Murray, R. W. (2000). *Accounts of Chemical Research, 33*, 27–36.
83. Paciotti, G. F., Myer, L., Weinreich, D., Goia, D., Pavel, N., McLaughlin, R. E., et al. (2004). *Drug delivery, 11*, 169–183.
84. Paciotti, G. F., Kingston, D. G. I., & Tamarkin, L. (2006). *Drug development research, 67*, 47–54.
85. Hostetler, M. J., Wingate, J. E., Zhong, C. J., Harris, J. E., Vachet, R. W., Clark, M. R., et al. (1998). *Langmuir, 14*, 17–30.
86. Ghosh, P., Han, G., De, M., Kim, C. K., & Rotello, V. M. (2008). *Advanced Drug Delivery Reviews, 60*, 1307–1315.
87. Oishi, M., Nakaogami, J., Ishii, T., & Nagasaki, Y. (2006). *Chemistry Letters, 35*, 1046–1047.
88. Bhumkar, D. R., Joshi, H. M., Sastry, M., & Pokharkar, V. B. (2007). *Pharmaceutical Research, 24*, 1415–1426.

89. Li, W., Huang, Z., MacKay, J. A., Grube, S., & Szoka, F. C. (2005). *The Journal of Gene Medicine, 7*, 67–79.
90. Polizzi, M. A., Stasko, N. A., & Schoenfisch, M. H. (2007). *Langmuir, 23*, 4938–4943.
91. Han, G., You, C.-C., Kim, B.-J., Turingan, R. S., Forbes, N. S., Martin, C. T., et al. (2006). *Angewandte Chemie International Edition, 45*, 3165–3169.
92. Han, G., You, C. C., Kim, B., Turingan, R. S., Forbes, N. S., Martin, C. T., et al. (2006). *Angewandte Chemie, 118*, 3237–3241.
93. Grabinski, C., Schaeublin, N., Wijaya, A., D'Couto, H., Baxamusa, S. H., Hamad-Schifferli, K., et al. (2011). *ACS Nano, 5*, 2870–2879.
94. Kirui, D. K., Krishnan, S., Strickland, A. D., & Batt, C. A. (2011). *Macromolecular Bioscience, 11*, 779–788.
95. De Jong, W. H., Hagens, W. I., Krystek, P., Burger, M. C., Sips, A. J. A. M., & Geertsma, R. E. (2008). *Biomaterials, 29*, 1912–1919.
96. Pan, Y., Neuss, S., Leifert, A., Fischler, M., Wen, F., Simon, U., et al. (2007). *Small, 3*, 1941–1949.
97. Lin, J., Zhang, H., Chen, Z., & Zheng, Y. (2010). *ACS Nano, 4*, 5421–5429.
98. Connor, E. E., Mwamuka, J., Gole, A., Murphy, C. J., & Wyatt, M. D. (2005). *Small, 1*, 325–327.
99. Pernodet, N., Fang, X., Sun, Y., Bakhtina, A., Ramakrishnan, A., Sokolov, J., et al. (2006). *Small, 2*, 766–773.
100. Shukla, R., Bansal, V., Chaudhary, M., Basu, A., Bhonde, R. R., & Sastry, M. (2005). *Langmuir, 21*, 10644–10654.
101. Rayavarapu, R. G., Petersen, W., Hartsuiker, L., Chin, P., Janssen, H., van Leeuwen, F. W. B., et al. (2010). *Nanotechnology, 21*, 145101–145110.
102. Chen, Y. S., Hung, Y. C., Liau, I., & Huang, G. S. (2009). *Nanoscale research letters, 4*, 858–864.
103. Cho, W. S., Cho, M., Jeong, J., Choi, M., Cho, H. Y., Han, B. S., et al. (2009). *Toxicology and Applied Pharmacology, 236*, 16–24.
104. Cho, W. S., Kim, S., Han, B. S., Son, W. C., & Jeong, J. (2009). *Toxicology letters, 191*, 96–102.
105. Balasubramanian, S. K., Jittiwat, J., Manikandan, J., Ong, C.-N., Yu, L. E., & Ong, W.-Y. (2010). *Biomaterials, 31*, 2034–2042.